Xue and Kang
Journal of Analytical Science and Technology (2024) 15:30
https://doi.org/10.1186/s40543-024-00443-3

Journal of Analytical Science and Technology

RESEARCH ARTICLE

Open Access

Target recognition-initiated allosteric probe-based multiple signal amplification strategy for sensitive and direct *Pseudomonas aeruginosa* detection

Kun Xue[1] and Shuhong Kang[2*]

Abstract

Pseudomonas aeruginosa (*P. aeruginosa*), a kind of gram-negative pathogenic bacteria, are causative agents of severe infections, such as lower respiratory tract infections in children and cancers. Detecting low levels of *P. aeruginosa* in clinical samples in an easy-to-operate manner is highly desired but still poses a problem. Herein, we established a target recognition-initiated allosteric probe-based multiple signal amplification strategy for sensitive detection of *P. aeruginosa* in a wash-free way. This approach involves the allosteric probe's accurate recognition and binding to target *P. aeruginosa*, leading to subsequent multiple-cycle amplification. Afterward, the amplified products were translated to induce the aggregation of gold nanoparticles (AuNPs), resulting in color variations. The utilization of the allosteric probe, which is integrated with the aptamer sequences, enables wash-free detection of *P. aeruginosa*. Taking the merit of multiple signal amplification process, the suggested method showed a strong linear response to the extracted *P. aeruginosa* within a concentration range of 10–10^5 cfu/mL, with a low limit of detection for individual *P. aeruginosa* detection. The proposed technique has considerable clinical promise for early disease diagnosis because to its high sensitivity and wash-free simplicity.

Keywords *Pseudomonas aeruginosa* (*P. aeruginosa*), Allosteric probe, Gold nanoparticles (AuNPs), Catalytic hairpin assembly (CHA)

Introduction

Gram-negative pathogenic bacteria, including *Pseudomonas aeruginosa* (*P. aeruginosa*), are able to inhabit both land and water settings (Camus et al. 2021; Haussler 2010; Mielko et al. 2019). The bacteria are causative agents of severe infections, including malignancy and lower respiratory tract infections in children (Qi et al. 2018; Yang et al. 2021), even at low concentrations. *P. aeruginosa* thrives in areas with low nutrition and humidity (Andonova and Urumova 2013; Ramos et al. 2013), such as medical and hospital equipment. Moreover, it exhibits resistance to antibiotics and antimicrobials because of biofilm development and the limited permeability of the outer membrane (Thi et al. 2020), respectively. This renders it a subject of investigation in numerous scientific domains, such as the swift detection or identification of substances within hospital settings.

Various techniques, including conventional bacterial culture (Li et al. 2022; Zheng et al. 2020) and immunological approach (ELISA) (Granstrom et al. 1985), can detect *P. aeruginosa*. However, these procedures are typically slow, expensive, and lack quantifiable outcomes.

*Correspondence:
Shuhong Kang
18991733609@163.com
[1] Pediatric Respiratory Department, Baoji Maternal and Child Health Hospital, Baoji City 721000, Shaanxi Province, China
[2] Pediatric Infectious Disease Department, Baoji Maternal and Child Health Hospital, No. 15 Jinger Street, Weibin District, Baoji City 721000, Shaanxi Province, China

Polymerase chain reaction (PCR)-based approaches have gained significant attention in detecting *P. aeruginosa* due to their effective gene fragment amplification, and are commonly utilized in clinical settings (Mangiaterra et al. 2018; Tang et al. 2014; Zhong and He 2019). PCR-based approaches have limitations such as complex primer design, the need for equipment for heat cycles, and the tedious and time-consuming steps of lysing the *P. aeruginosa* membrane and extracting genetic material. Thus, rapid and affordable identification of *P. aeruginosa* is crucial for human health and food safety. Rapid *P. aeruginosa* detection has been the subject of only a limited number of recent studies. Aptamers are distinguished in this realm for their selectivity toward the target and their ease of conjugation with nanomaterials (Khatami et al. 2022; Gutierrez-Santana and Coria-Jimenez 2024). Aptamers have been used for direct detection of *P. aeruginosa* by methods like fluorescence assay, colorimetry, and electrochemical approaches. Colorimetric approaches can provide detection results by color changes that are visible to the human eye, making portable bacterium detection easier (Das et al. 2019; Liu et al. 2023). A method integrating the aptamer with gold nanoparticles have been employed to detect *P. aeruginosa*, in which *P. aeruginosa* was detected after 5 h for concentrations from 10^8 to 10^5 cfu/mL, being 10^5 and 10^4 cfu/mL the detection limit for color change by the naked eye and UV–Vis spectrometry, respectively (Schmitz et al. 2023). However, colorimetric assays sometimes lack sufficient sensitivity to meet the increased demand for detecting low concentrations of *P. aeruginosa*.

The sensitivity of the colorimetric *P. aeruginosa* detection methods has been enhanced by incorporating several signal amplification procedures (Yuan et al. 2022; Kuhnemund et al. 2017; Xie et al. 2022). The polymerase/endonuclease-assisted chain reaction is a signal amplification strategy that efficiently produces single-stranded DNA sequences (Zhao et al. 2020). It is commonly utilized in the development of new biosensors. Further enhancement of the sensitivity of the polymerase/endonuclease-assisted chain reaction is required.

Utilizing a target recognition-initiated allosteric probe-based multiple signal amplification strategy, this research endeavors to devise a technique for the rapid, selective, and sensitive detection of *P. aeruginosa*. The aptamer has been incorporated into the allosteric probe, with the aptamer acting as the bio-recognition element for *P. aeruginosa*. Aptamer binds to the target bacteria, causing allosterism of the probe and exposure of the "1" fragment, which triggers the subsequent quadruple signal amplification process. Ultimately, the aggregated gold nanoparticles (AuNPs) induce the observed color changes.

Experimental

Material and reagents

Each reagent was at least of analytical quality. The supplier from Shanghai Boao Bio-Science & Technology Company (Shanghai, China) supplied the bovine serum albumin (BSA). The details of the oligonucleotides, which were purified and synthesized by Shanghai Sangon Biological Science & Technology Company (Shanghai, China), are shown in Table S1. The aptamer and FAM-cDNA were dissolved in deionized water and stored at -− 20 °C before use. The water utilized in the experiments was purified using an ELGA system. The culturing procedures and the origin of the microorganisms were provided in the supporting information.

Allosteric probe-based bacteria recognition.

Target recognition: The synthesized probes were dissolved in 1 × NEBuffer (pH, 7.9) and consisted of 10 mM $MgCl_2$, 50 mM NaCl, 10 mM Tris–HCl, and 1 mM DTT. The extracted *P. aeruginosa* were then quantified via colony counting method and were diluted to various concentrations prior to detection. Following this, 2.5 μL of *P. aeruginosa* was incubated at room temperature for 30 min with 5 μL of the synthesized florescent allosteric probe (1 μM), 5 μL of assist probe (5 μM). Fluorescence signals were subsequently detected using a Hitachi fluorescence spectrophotometer F-7100 (Beijing, China) both prior to and subsequent to the *P. aeruginosa* mixing procedure.

Polymerase/endonuclease-assisted chain reaction: Following this, dNTP was added to a buffer solution comprising spermidine (2 mM), Tris–HCl (40 mM), dithiothreitol (1 mM), and $MgCl_2$ (11 mM) with a pH of 7.9 and a temperature of 37 °C for a duration of 30 min. The Nt.BbvCI nicking enzyme was diluted in a solution of 50% glycerol, 10 mM Tris–HCl, 50 mM KCl, 1 mM DTT, 0.1 mM EDTA, and 200 μg/mL BSA. Subsequently, for the polymerase/endonuclease-assisted chain reaction, the mixture was combined with 4 μL of dNTP, 2 μL of Klenow DNA polymerase, and 1 μL of Nt.BbvCI nicking enzyme.

Color reaction: The previously mentioned mixture, which includes the generated "m" sequences, is combined with H1 probe@AuNPs and H2 probe@AuNPs. After 60 min of incubation at room temperature, the signal was observed with the naked eye. In addition, UV–vis spectra of the amplification were acquired through the utilization of a BioSpec-nano UV–vis spectrophotometer.

Data analysis

The results of each test, which were conducted independently in at least triplicate, were presented as the mean ± standard deviation (SD). The information was subsequently depicted graphically using GraphPad Prism

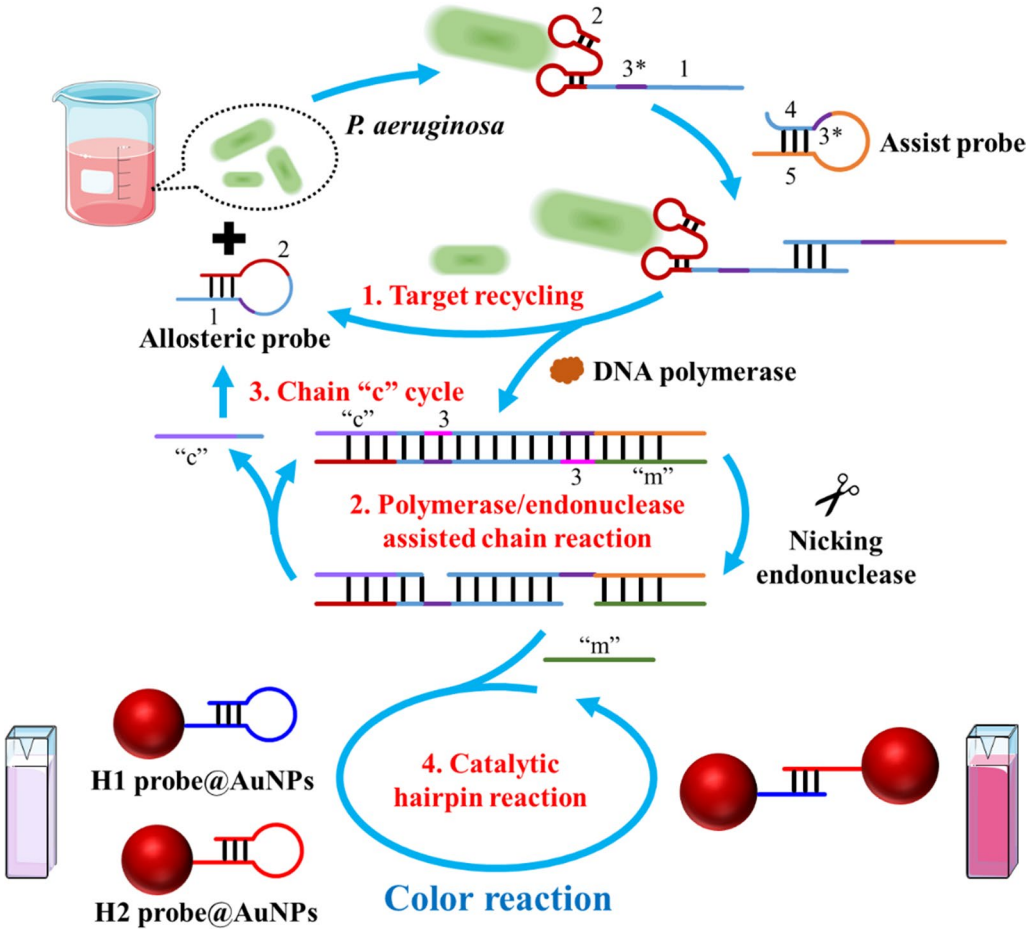

Scheme 1. Working mechanism of the proposed colorimetric approach for sensitive *P. aeruginosa* detection

8.0. Student's t test was applied to analyze comparisons between two groups. Differences were considered significant at values of $P < 0.05$.

Results and discussion

The working mechanism of the approach for sensitive and colorimetric *P. aeruginosa* detection

The working mechanism of the proposed telomerase activity-sensing strategy is depicted in Scheme 1. To obtain ultrasensitive *P. aeruginosa* identification, four active components are employed: allosteric probe, assist probe, H1 probe@AuNPs, and H2 probe@AuNPs. The allosteric probe is an ssDNA molecule composed of three functional domains: *P. aeruginosa* aptamer domain for target bacteria identification ("2"), H1 initiator domain ("1") for hybridization chain reaction, and a nicking domain ("3*"). By hybridization between the two complementary parts in the allosteric probe, a hairpin structure is eventually formed after annealing. The assist probe is composed by three domains: "1" binding site domain ("4"), a nicking domain ("3*"), and "5". In the presence of target bacterial, the "2" fragment binds with the surface protein, and thus the "1" fragment is exposed. The "1" fragment binds with the "4" fragment to unfold the assist probe. With the assistance of the DNA polymerase, a double-stranded DNA product was produced containing transcribed "3" fragment, "c" fragment, and "m" fragment. Meanwhile, the target bacteria are released from the allosteric probe and can bind with a next allosteric probe (1. Target recycling). Notably, when recognizing the complementary sequence ("3": 5′-CCTCAGC-3′) of the nicking domain, the nicking enzyme (Nt.BbvCI) will cut it to generate a nick. Under the cooperation of the polymerase and endonuclease, polymerase/endonuclease-assisted chain reaction was initiated to produce numerous "c" and "m" sequences (2. Polymerase/endonuclease-assisted chain reaction). The "c" sequence unfolds a next allosteric probe, forming the third signal amplification (3. Chain "c" cycle). The "m" sequence mediates the catalytic hairpin assembly (CHA) of the H1 probe@AuNPs and H2 probe@AuNPs (4. CHA process), resulting in the aggregation of AuNPs and the color changes.

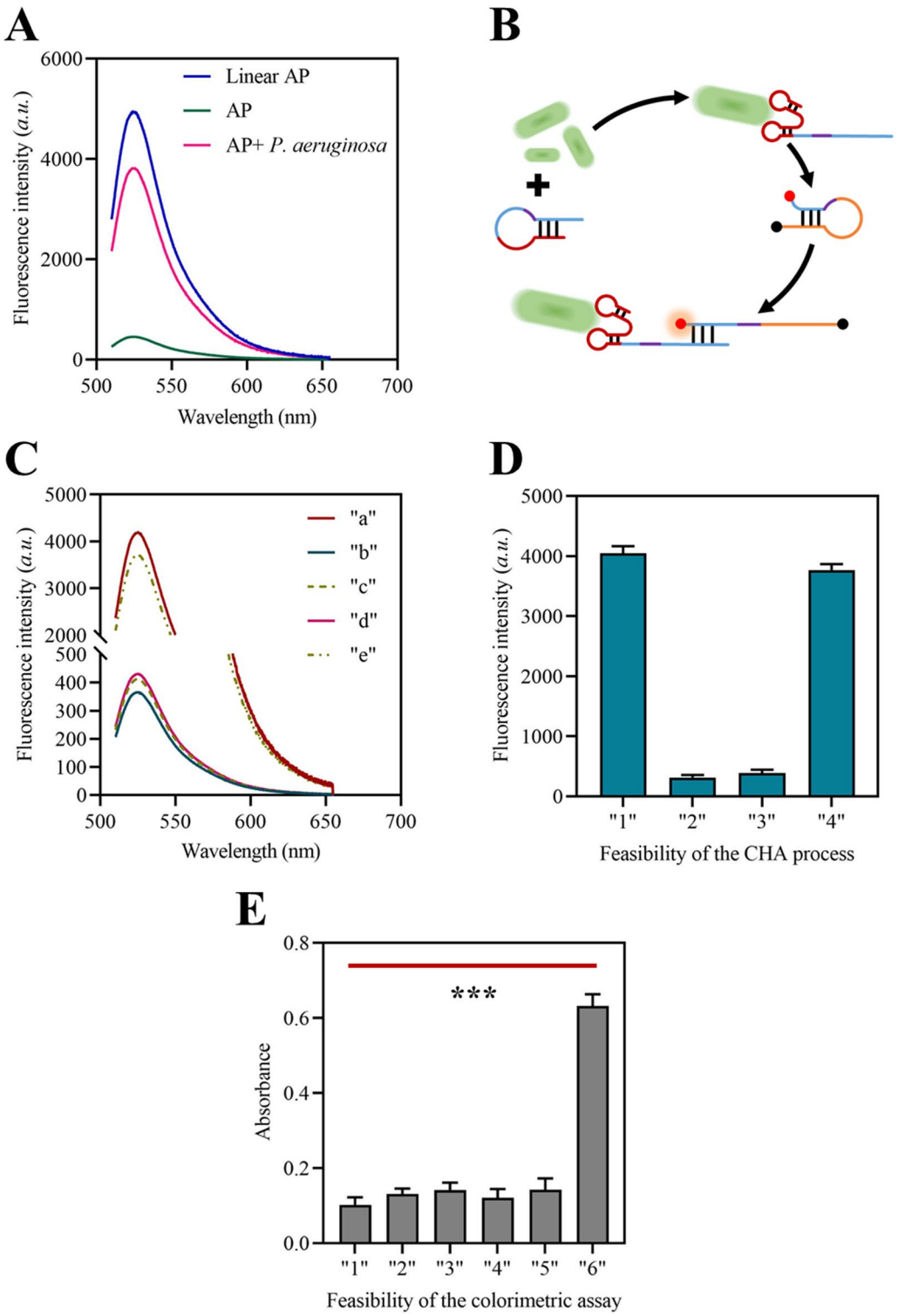

Fig. 1 Assembly of the allosteric probe and feasibility of the approach. **A** Fluorescence spectrum of the FAM labeled allosteric probe before and after assembly. AP, allosteric probe. **B** Schematic illustration of the fluorescence assay to test the target recognition-based disassociation of assist probe. **C** Fluorescence spectrum of the FAM labeled assist probe when detecting *P. aeruginosa*. **D** Fluorescence intensities of the FAM labeled H2 probe during the CHA process. **E** Absorbance of the approach when essential experiment components were existed or not

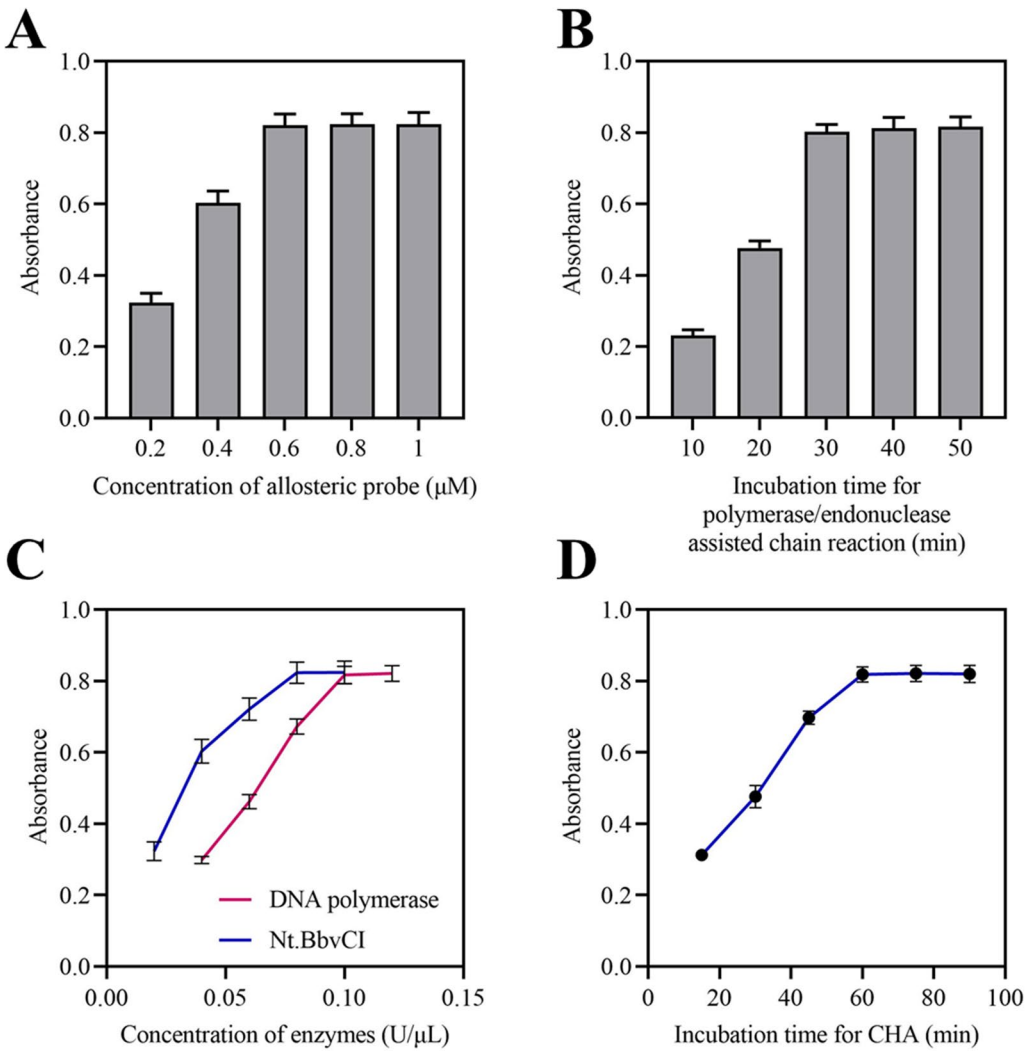

Fig. 2 Optimization of the experimental parameters. The absorbance values of the approach with different concentrations of allosteric probe (**A**), different incubation time for the polymerase/endonuclease-assisted chain reaction (**B**), different concentrations of the enzymes (**C**), different incubation time for the CHA process

Assembly of the allosteric probe and feasibility of the approach

In order to validate that the activate configuration of the designed allosteric probe can be selectively triggered by *P. aeruginosa* recognition, the allosteric probe is initially synthesized with a hairpin configuration that quenches the initial fluorescence of a fluorescence (FAM) labeled at its terminals by BHQ-1. The fluorescence signal of the synthesized allosteric probe recovers upon recognition and binding to the extracted *P. aeruginosa* (Fig. A), indicating that the allosteric probe binds with *P. aeruginosa* and transitions to its active configuration. As depicted in Fig. 1B, the fluorescence assay is conducted utilizing synthesized probes (F-assist-probe) that have internal labeling at the 5′ end and FAM labeled at the 3′ end. Furthermore, the outcome (Fig. 1C) illustrates a hairpin assembly that was effectively initiated in response to *P. aeruginosa* recognition. To evaluate the CHA process initiated by the "m" sequences, the two termini of the H2 probe were labeled with FAM and BHQ, respectively. The peak fluorescent value was considerably greater than that of the control group, as shown in Fig. 1D; this finding validates the effectiveness of the CHA process. The color alterations exhibited by the AuNPs in Fig. 1E served as evidence that the entire sensing system was functional in the presence of all necessary components.

Optimization of experimental parameters

To enhance the efficacy of the assay, we subsequently optimized the concentrations of the designed allosteric probe, which is crucial in target recognition and

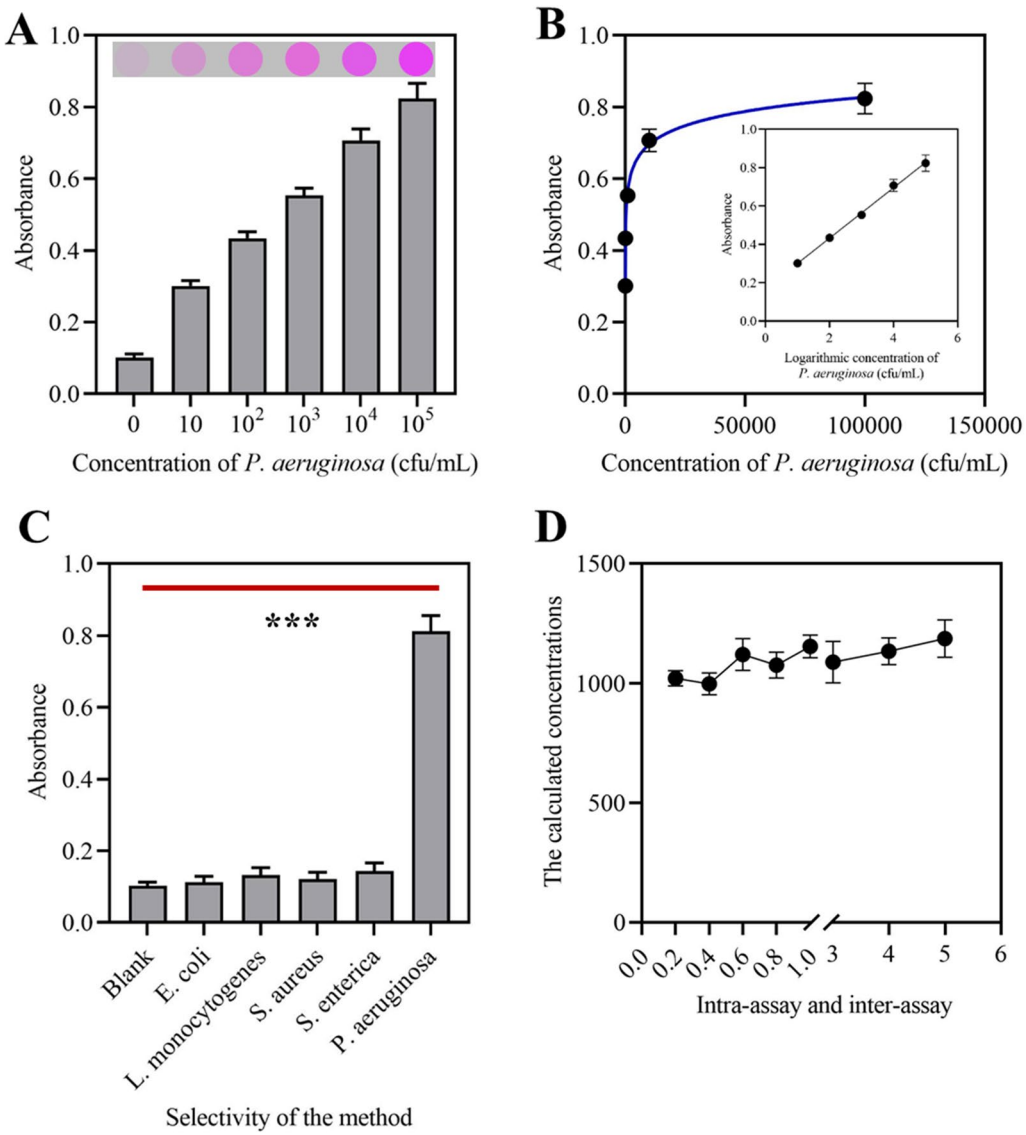

Fig. 3 Analytical performance of the approach. **A** The absorbance values of the approach when detecting different concentrations of target bacteria. **B** Correlation between the absorbance values and the concentration of the target bacteria. **C** Absorbance of the method when detecting different bacteria. **D** The calculated concentration of *P. aeruginosa* from different batches of samples

mediating the disassociation of assist probe. As the concentration of the allosteric probe increases until it reaches 0.6 μM, the absorbance rises; at a significantly higher concentration, it begins to decline (Fig. 2A). Our initial hypothesis was that an increase in the concentration of the allosteric probe would result in a corresponding enhancement in the reaction rate of the catalytic process. On the contrary, an overabundance of allosteric probe leads to a reduction in amplification efficiency. This phenomenon could potentially be attributed to the formation of dimers, which is in turn obstructed by sequence binding. As a result, 0.6 μM is determined to be the optimal concentration of the allosteric probe for the subsequent investigations.

We optimized the incubation period for polymerase/endonuclease-assisted chain reaction. Figure 2B demonstrates that there is no further increase in absorbance for the polymerase/endonuclease-assisted chain reaction after a 30 min of incubation. We then confirmed the optimal concentration of the two enzymes, including the DNA polymerase and Nt.BbvCI nicking enzyme. The ideal concentrations of DNA polymerase and Nt.BbvCI nicking enzyme are 0.1 and 0.08 U/μL, respectively, as shown in Fig. 2C.

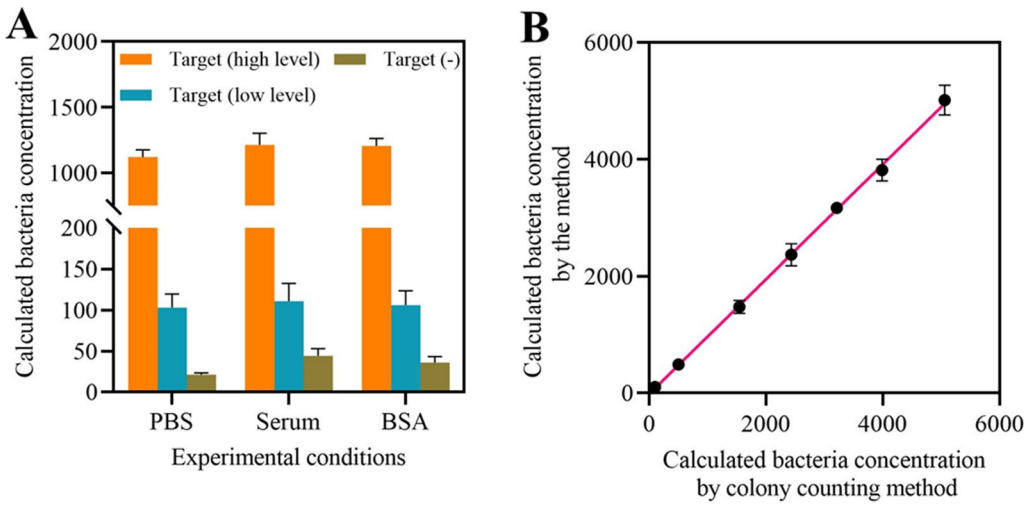

Fig. 4 Clinical application of the approach. **A** The calculated bacteria concentrations by the method from samples with different buffer solutions. **B** Correlation between the calculated bacteria concentrations by the method and by the colony counting method

We optimized the incubation period of the CHA-based color reaction by evaluating changes in absorbance values over time. Figure 2D shows that the absorbance rises over time, reaching its highest point after 60 min of incubation. Extending the incubation period by a further 60 min did not result in any further increase in absorbance. This indicates that a 60 min of incubation is sufficient for the CHA process to attain reaction equilibrium.

Detective performance of the approach

Quantitative analysis was conducted by measuring the absorbance of the aggregated AuNPs in the supernatant. Figure 3A demonstrates that the absorbance increases in direct proportion to the logarithm of *P. aeruginosa* concentration within the range of 10 cfu/mL to 10^5 cfu/mL. The calibration curve shows a regression equation of $F=0.1317*\lg C+0.1685$ with a determination coefficient of $R^2=0.9845$. Here, F represents the absorbance intensity of the AuNPs, and C (cfu/mL) denotes the concentration of *P. aeruginosa* (Fig. 3B). The detection limit (LOD) of 3 cfu/mL is determined by dividing 3 times the standard deviation of the blanks by the slope of the linear calibration plot equation (LOD = 3SD/slope).

In order to assess the method's specificity, *P. aeruginosa* (10^4 cfu/mL) was identified as the positive control sample, while four other pathogens of equivalent concentration (*E. coli* O157:H7, *L. monocytogenes*, *S. aureus*, and *S. enterica*) were detected as negative controls. The allosteric probe was used to incubate these samples under identical conditions. *P. aeruginosa* exhibits a conspicuous augmentation in absorbance, as illustrated in Fig. 3C. In comparison with *P. aeruginosa*, the absorbance values of the four negative controls are below 0.15. The results indicate that the aptamer-based method targets *P. aeruginosa* with high specificity and selectivity.

The parallel samples were assessed using the same batch and various batches of method components to assess the method's reliability. The approach demonstrates good consistency as both the intra-assay and inter-assay relative standard deviations (RSDs) are below 4.87% (Fig. 3D).

Real sample analysis

PBS buffer, serum from a commercial source, and BSA solution were utilized to confirm the method's viability. To confirm the method's effectiveness in detecting *P. aeruginosa* in real samples, spiked PBS buffer solution, commercial serum, and BSA solution containing 1000 cfu/mL of *P. aeruginosa* were utilized as test samples. Figure 4A displays the average recoveries of the spiked samples, which vary from 91.0% to 110% with analytical precision meeting the criteria (RSD ≤ 6.6%). The findings suggest that the developed approach is capable of identifying *P. aeruginosa* in actual samples. To enhance detection accuracy, the concentration of the target bacterium was varied, and both the classic colony counting approach and the established method were used to detect *P. aeruginosa*. Figure 4B displays the detected concentrations from both methods, showing a high level of consistency and accuracy.

Conclusion

We present a sensitive, wash-free, and reliable colorimetric approach for detecting *P. aeruginosa* using an allosteric probe-initiated multiple amplification strategy. The proposed method possesses the following advantages,

including (i) the elegant design of the allosteric probe integrated the capability of specific target recognition and initiating subsequent signal amplification, enabling target bacteria detection in a wash-free manner; (ii) quadruple signal amplification processes are included in the method, endowing the method with a high sensitivity; (iii) CHA process mediated aggregation of the AuNPs resulted in the color changes, which possesses a wider application sceneries, even in resource-limited countries. With its high sensitivity guaranteed by the four signal cycles, the proposed method is distinguished by its user-friendliness and a high reliability in clinical samples detection, which is superior or comparable to most of the former methods (Table S2). This approach showed a broad detection range spanning five orders of magnitudes without requiring ultracentrifugation. However, the proposed method could be applied for the *P. aeruginosa* (ATCC 27853) detection, which limits its further application in detecting other bacteria. In the future, we will focus on developing a versatile platform for various bacteria detection. We anticipate that this concept will offer a novel method for analyzing biological processes in live systems, hence aiding in the diagnosis of various human disorders.

Supplementary Information

The online version contains supplementary material available at https://doi.org/10.1186/s40543-024-00443-3.

Additional file 1.

Acknowledgements
We feel so appreciated for the financial support from Baoji Maternal and Child Health Hospital. The authors have no other relevant affiliations or financial involvement with any organization or entity with a financial interest in or financial conflict with the subject matter or materials discussed in the manuscript apart from those disclosed.

Author contributions
S.K. is responsible for study conception and design; K.X. is responsible for acquisition of data, data analysis, and drafting the manuscript.

Funding
Not applicable.

Availability of data and materials
All experimental data are presented in the article or additional file.

Declarations

Ethics approval and consent to participate
The manuscript does not contain clinical or trial studies on patients, humans, or animals.

Competing interests
The authors declare that they have no competing interests.

Received: 3 March 2024 Accepted: 8 May 2024
Published online: 16 May 2024

References

Andonova M, Urumova V. Immune surveillance mechanisms of the skin against the stealth infection strategy of *Pseudomonas aeruginosa*-review. Comp Immunol Microbiol Infect Dis. 2013;36(5):433–48.
Camus L, Vandenesch F, Moreau K. From genotype to phenotype: adaptations of *Pseudomonas aeruginosa* to the cystic fibrosis environment. Microb Genom. 2021;7(3):000513.
Das R, Dhiman A, Kapil A, Bansal V, Sharma TK. Aptamer-mediated colorimetric and electrochemical detection of *Pseudomonas aeruginosa* utilizing peroxidase-mimic activity of gold NanoZyme. Anal Bioanal Chem. 2019;411(6):1229–38.
Granstrom M, Wretlind B, Markman B, Pavlovskis OR, Vasil ML. Enzyme-linked immunosorbent assay for detection of antibodies to *Pseudomonas aeruginosa* exoproteins. Eur J Clin Microbiol. 1985;4(2):197–200.
Gutierrez-Santana JC, Coria-Jimenez VR. Diagnosis and therapeutic strategies based on nucleic acid aptamers selected against *Pseudomonas aeruginosa*: the challenge of cystic fibrosis. ChemMedChem. 2024;19(2):e202300544.
Haussler S. Multicellular signalling and growth of *Pseudomonas aeruginosa*. Int J Med Microbiol. 2010;300(8):544–8.
Khatami SH, Karami S, Siahkouhi HR, Taheri-Anganeh M, Fathi J, Aghazadeh Ghadim MB, Taghvimi S, Shabaninejad Z, Tondro G, Karami N, Dolatshah L, Soltani Fard E, Movahedpour A, Darvishi MH. Aptamer-based biosensors for Pseudomonas aeruginosa detection. Mol Cell Probes. 2022;66:101865.
Kuhnemund M, Hernandez-Neuta I, Sharif MI, Cornaglia M, Gijs MAM, Nilsson M. Sensitive and inexpensive digital DNA analysis by microfluidic enrichment of rolling circle amplified single-molecules. Nucleic Acids Res. 2017;45(8): e59.
Li Y, Hu Y, Chen T, Chen Y, Li Y, Zhou H, Yang D. Advanced detection and sensing strategies of *Pseudomonas aeruginosa* and quorum sensing biomarkers: a review. Talanta. 2022;240:123210.
Liu J, Lu D, Wang J. A simple, sensitive and colorimetric assay for *Pseudomonas aeruginosa* infection analysis. Biotechniques. 2023;75(5):210–7.
Mangiaterra G, Amiri M, Di Cesare A, Pasquaroli S, Manso E, Cirilli N, Citterio B, Vignaroli C, Biavasco F. Detection of viable but non-culturable Pseudomonas aeruginosa in cystic fibrosis by qPCR: a validation study. BMC Infect Dis. 2018;18(1):701.
Mielko KA, Jablonski SJ, Milczewska J, Sands D, Lukaszewicz M, Mlynarz P. Metabolomic studies of *Pseudomonas aeruginosa*. World J Microbiol Biotechnol. 2019;35(11):178.
Qi X, Qu H, Yang D, Zhou L, He YW, Yu Y, Qu J, Liu J. Lower respiratory tract microbial composition was diversified in *Pseudomonas aeruginosa* ventilator-associated pneumonia patients. Respir Res. 2018;19(1):139.
Ramos GP, Rocha JL, Tuon FF. Seasonal humidity may influence *Pseudomonas aeruginosa* hospital-acquired infection rates. Int J Infect Dis. 2013;17(9):e757–61.
Schmitz FRW, Cesca K, Valerio A, de Oliveira D, Hotza D. Colorimetric detection of *Pseudomonas aeruginosa* by aptamer-functionalized gold nanoparticles. Appl Microbiol Biotechnol. 2023;107(1):71–80.
Tang Y, Ali Z, Zou J, Yang K, Mou X, Li Z, Deng Y, Lu Z, Ma C, Shah MA, Elingarami S, Yang H, He N. Detection of Pseudomonas aeruginosa based on magnetic enrichment and nested PCR. J Nanosci Nanotechnol. 2014;14(7):4886–90.
Thi MTT, Wibowo D, Rehm BHA. Pseudomonas aeruginosa Biofilms. Int J Mol Sci. 2020;21(22):8671.
Xie Y, Xie G, Yuan J, Zhang J, Yang Y, Yao Y, Wu Y, Bai D, Chen K, Li B, Song L, Chen H. A novel fluorescence biosensor based on double-stranded DNA branch migration-induced HCR and DNAzyme feedback circuit for sensitive detection of Pseudomonas aeruginosa (clean version). Anal Chim Acta. 2022;1232: 340449.
Yang X, Lai Y, Li C, Yang J, Jia M, Sheng J. Molecular epidemiology of *Pseudomonas aeruginosa* isolated from lower respiratory tract of ICU patients. Braz J Biol. 2021;81(2):351–60.
Yuan W, Wang X, Sun Z, Liu F, Wang D. A synergistic dual-channel sensor for ultrasensitive detection of *Pseudomonas aeruginosa* by DNA nanostructure and G-quadruplex. Biosensors (basel). 2022;13(1):24.
Zhao X, Zeng L, Mei Q, Luo Y. Allosteric probe-initiated wash-free method for sensitive extracellular vesicle detection through dual cycle-assisted CRISPR-Cas12a. ACS Sens. 2020;5(7):2239–46.

Zheng X, Gao S, Wu J, Hu X. Recent advances in aptamer-based biosensors for detection of *Pseudomonas aeruginosa*. Front Microbiol. 2020;11:605229.
Zhong D, He W. Detection of Pseudomonas aeruginosa in the Skin by Immunomagnetic Isolation and Real-Time Quantitative PCR. J Nanosci Nanotechnol. 2019;19(9):5517–21.

Publisher's Note